



HOKKAIDO UNIVERSITY

Title	Mechanisms of Multiple Cracking and Fracture of DFRCC under Fatigue Flexure
Author(s)	Takashi, Matsumoto; Peerapong, Suthiwarapirak; Kanda, Tetsushi
Citation	Journal of Advanced Concrete Technology, 1(3), 299-306
Issue Date	2003-11
Doc URL	https://hdl.handle.net/2115/47375
Type	journal article
File Information	JACT_1_299-306.pdf



Mechanisms of Multiple Cracking and Fracture of DFRCC under Fatigue Flexure

Takashi Matsumoto¹, Peerapong Suthiwarapirak² and Tetsushi Kanda³

Received 28 January 2003, accepted 26 April 2003

Abstract

This paper presents an experimental study on the flexural fatigue characteristics of PVA-ECC and PE-ECC. The ECCs showed a unique S-N relationship and exhibited the development of multiple cracks even under fatigue loading. The development of multiple cracks was found to be dependent on fatigue stress levels, and the mechanism is discussed in reference to the static multiple cracking mechanism. The difference between the two ECCs appeared especially in the deformation capacity under fatigue loading. The deformation is shown to be affected by the number of cracks as well as the crack width, where the fracture mechanism of a bridged crack is related to either fiber rupture or fiber pullout.

1. Introduction

This paper presents an experimental study on the flexural fatigue characteristics of DFRCCs (Ductile Fiber Reinforced Cementitious Composites), particularly two types of ECCs (Engineered Cementitious Composites), and discusses the mechanisms of multiple cracking and fracture of the ECCs under flexural fatigue.

DFRCCs are defined as a cementitious composite material reinforced with fibers that shows multiple cracking characteristics under bending stress and whose ductility at bending, tension, and compression failure is drastically improved (Rokugo et al. 2002). These characteristics and ductility of DFRCCs can be clearly demonstrated by ECCs, and furthermore ECCs can exhibit strain hardening and multiple cracking characteristics even under uniaxial tensile stress. Therefore, the investigation on the mechanisms of multiple cracking and fracture is carried out with ECCs in this paper.

Fatigue characteristics of ECCs are important because their unique characteristics, such as multiple cracking and strain hardening under monotonic tension or flexure, can be further exploited to achieve long-term durability for fatigue intensive structures.

However, fatigue characteristics of ECCs have not been fully clarified to date. For example, the process of multiple cracking and the fracture mechanism have not been investigated under fatigue loading, although there have been several studies under static loading (Li et al. 1992; Kanda et al. 1999; Maalej et al. 1994). Therefore, they need to be clarified to obtain the principles for material design as well as structural application.

This paper focuses on the two types of ECCs under

flexural fatigue. These ECCs were tested under four-point flexural fatigue so as to construct stress-life (S-N) relationships and to investigate the process of multiple cracking as well as the fracture mechanism. Based on these experimental observations, the mechanisms of multiple cracking and fracture of these ECCs are discussed.

2. Experimental program

2.1 Materials and specimens

Static and fatigue flexure experiments were conducted for two types of ECCs: one reinforced with polyvinyl alcohol (PVA) fibers and the other with polyethylene (PE) fibers. These two ECCs are referred to as PVA-ECC and PE-ECC, respectively. The properties of these two fiber types are shown in **Table 1**. The mix proportions are the same for the two ECCs, and are listed in **Table 2**.

A wet mixed shotcrete method was applied to fabricate the beam specimens with depth of 100 mm, thickness of 100 mm, and length of 400 mm (Kanda et al. 2001b). 22 specimens for PVA-ECC and 15 specimens for PE-ECC were shotcreted into forms. After fabrication, all specimens were moist cured under a constant temperature of 20°C and relative humidity of 60%. The

Table 1 Fiber properties (Kanda et al. 2001a).

	PVA-ECC	PE-ECC
Type	PVA fiber	PE fiber
Length (mm)	12	8
Diameter (μm)	37.7	12
Elastic modulus (GPa)	36.7	75.0
Volume fraction (%)	1.9	1.5
Tensile strength (MPa)	1610	2790
Interfacial bond strength (MPa)	2.01	0.66

¹Associate Professor, Department of Civil Engineering, University of Tokyo, Japan.

E-mail: matsumoto@ohriki.t.u-tokyo.ac.jp

²Graduate Student, Department of Civil Engineering, University of Tokyo, Japan.

³Kajima Technical Research Institute, Japan.

Table 2 Mix proportion of PVA-ECC and PE-ECC
(Kanda et al. 2001b).

Water/Binder	Sand/Binder r	Water (kg/m ³)
0.32	0.42	382

age of the specimens at testing was at least two months, so as to alleviate the effect of initial hydration development.

2.2 Testing procedures

The flexural beams were tested with a 200 kN capacity feedback controlled loading machine. Static tests were carried out under displacement control, and fatigue tests under load control. Both static and fatigue tests were conducted under four-point flexure, with the specimens simply supported with a clear span of 300 mm (Fig. 1).

Static flexural tests were conducted before the flexural fatigue tests. The static flexural strengths of the two ECCs were determined by averaging the four results of PVA-ECC and the three results of PE-ECC, respectively. Based on the average static flexural strength, σ_{fuave} , the maximum fatigue stress levels, σ_{max} , were determined: five levels for PVA-ECC and four for PE-ECC.

(1) Static flexural tests

Static flexural tests were conducted in accordance with JCI Standards for Test Methods of Fiber Reinforced Concrete JCI-SF4 (1984). The tests were run under displacement control at a loading rate of 0.02 mm/s.

(2) Fatigue flexural tests

Flexural fatigue tests were run under load control. All the specimens were subjected to sinusoidal cyclic loading at 8 Hz frequency, and the ratio of the minimum stress level to the maximum stress level was set to 0.2 to avoid any impact and slip between the loading machine and the specimens during testing. The fastest possible frequency was chosen so that the aforementioned input would be executed accurately by the loading machine.

The fatigue loading sequence was as follows. In the

first cycle, the load was gradually increased to the maximum stress level in 50 seconds, and then the cyclic load was applied with 8 Hz sinusoidal waves. The tests were terminated either after fatigue failure took place or the number of cycles reached two million.

In order to construct the fatigue stress-life relationship, fatigue tests were conducted under five fatigue stress levels for PVA-ECC and four fatigue stress levels for PE-ECC. The fatigue stress level, S , is defined as the ratio of the maximum stress to the static flexural strength, and two to four specimens were assigned for each fatigue stress level. It should be noted that the total number of specimens is different between the two ECCs and also that the number of specimens at each stress level is rather limited from the viewpoint of tests started with the highest fatigue stress level ($S = 0.9$) for both types of ECCs. Based on the fatigue life results on the previous fatigue stress level, the next stress level was determined to obtain the entire S-N relationship. The determined fatigue stress levels are listed in Table 3.

(3) Data collection

Linear Variable Differential Transducers (LVDTs) were additionally used for deflection measurements. Two LVDTs were mounted on a steel frame that was attached to a beam specimen to avoid support and other deformations, and they measured the deflections of the specimen on both sides (Fig. 1).

Two sizes of π -shape displacement transducers (PI gauges) with gauge lengths of 100 mm (long) and 50 mm (short) were used to measure the deformation within the gauge length. One long PI gauge was attached to each side of the PVA-ECC specimens, while two short PI gauges were attached to each side of the PE-ECC specimens (Fig. 1). These transducers were attached at the bottom edge of the side faces of each specimen, and therefore they were supposed to measure the deformation of the tension face of the specimen. Furthermore, two short PI gauges attached in series were to detect the deformation localization that took place within either gauge length. In the experimental program, PVA-ECC specimens were tested first, and

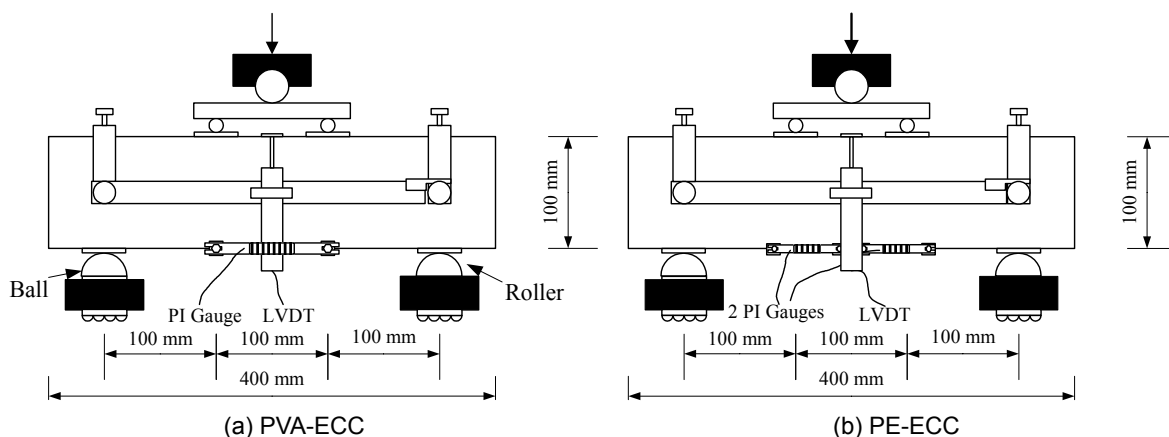


Fig. 1 Test setup.

Table 3 Number of specimens at each fatigue stress level.

Material	Level	1	2	3	4	5
PVA-ECC	S*	0.90	0.85	0.75	0.60	0.50
	N _s **	4	4	4	4	2
PE-ECC	S	0.90	0.80	0.70	0.60	
	N _s	3	3	3	3	

* S = $\sigma_{max}/\sigma_{fuave}$ = Fatigue stress level

** N_s = Number of specimens

PE-ECC specimens next with more detailed measurement. The observation of the deformation localization is reported elsewhere (Suthiwarapirak et al. 2003).

Microscopic observation was carried out to measure the crack opening displacement (COD) of a localized crack that led to the final failure of ECCs. At testing, all the specimens were painted white to facilitate microscopic and visual observations.

During fatigue loading, measurement data from the LVDTs and PI gauges were recorded at the maximum and minimum stress levels. Microscopic and visual observations were made at regular intervals and upon the event of cracking. The numbers of cycles at which cracks initiated and at which final failure took place were recorded.

3. Results

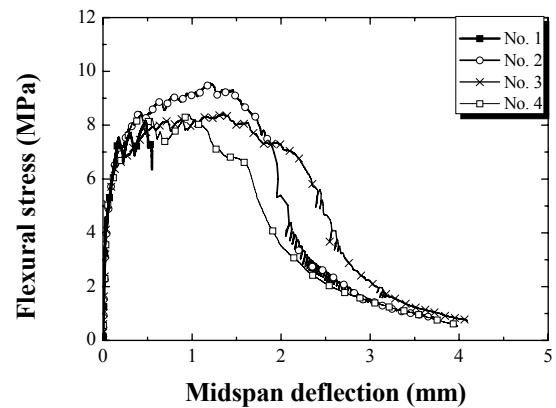
3.1 Static test results

Ultimate load, P_u, and flexural strength, σ_{fu} , of PVA-ECC and PE-ECC are summarized in Table 4, and average flexural strength, σ_{fuave} , is also included. Flexural strength is simply calculated with the elastic flexural beam formulation. Figure 2 shows flexural stress-midspan deflection relationships for all tested specimens. As shown in Table 4 and Fig. 2, both materials exhibit a typical ECC behavior in flexure. Namely, it was observed that the continuous rise in flexural stress after first cracking followed the initial elastic response. During this hardening, cracks were formed successively and distributed throughout the span until one of the cracks turned into a localized crack together with overall load decay. PE-ECC showed relatively higher

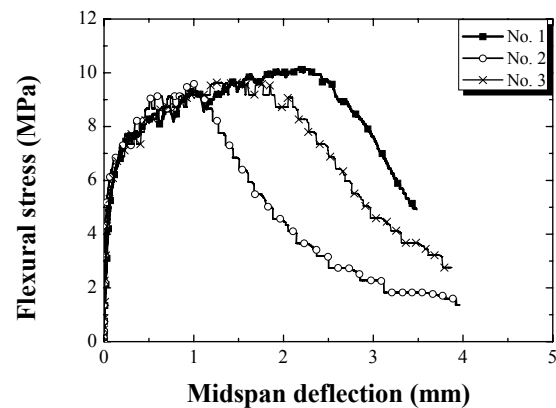
strength and deformation capacity than PVA-ECC.

Although the flexural stress-midspan deflection relationships do not differ considerably from each other, the characteristics of multiple cracks are slightly different between these two ECCs.

Figure 3 shows the crack patterns on the tension face of PVA-ECC beam specimens after static and fatigue tests, while Fig. 4 shows those of PE-ECC beam specimens. As shown in these figures, PVA-ECC formed a smaller number of multiple cracks compared to PE-ECC (Fig. 5). Therefore, the higher deformation capacity of PE-ECC originated from a larger number of cracks with smaller crack opening displacements. The difference is due to the fact that PVA-ECC is fiber rupture dominant,



(a) PVA-ECC



(b) PE-ECC

Fig. 2 Flexural stress-midspan deflection relationship.

Table 4 Results of static flexural tests.

Material	Specimen	Ultimate Load, P _u (kN)	Flexural Strength, σ_{fu} (MPa)	Average Flexural Strength, σ_{fuave} (MPa)
PVA-ECC	1	27.68	8.151	8.709
	2	32.70	9.556	
	3	28.65	8.421	
	4	28.52	8.385	
PE-ECC	1	34.69	10.304	9.927
	2	32.80	9.788	
	3	32.80	9.691	

while PE-ECC is fiber pull-out dominant. Although PVA-ECC has higher interfacial bond strength and longer fiber length, it has lower fiber strength than PE-ECC, leading to more fiber rupture on balance.

3.2 Fatigue test results

Figure 6 shows S-N relationships constructed based on the fatigue test results. The arrows indicate the specimens that reached two million cycles without failure. S-N relationships are shown for two ECCs together with a shotcrete type FRC (Fiber Reinforced Concrete) for comparison (Suthiwarapirak et al. 2003). **Figure 6 (a)** shows the relationship between fatigue stress and fatigue life. Overall, ECCs demonstrate superior fatigue strength performance for a given fatigue life requirement. It is interesting to note that ECCs exhibit a unique S-N relationship that resembles that of metallic materi-

als and can be characterized by a bi-linear relationship on a semi-log plot. On the other hand, FRC exhibits a typical S-N relationship that is represented by a linear relationship on the same plot. **Figure 6 (b)** shows a normalized S-N relationship where fatigue stress is divided by the static strength. It shows that such a unique S-N relationship is due to the fact that the ECCs recorded relatively longer fatigue lives at higher fatigue stress levels. However this figure also shows that the fatigue life of ECCs tended to be equivalent or shorter than that of FRC at lower fatigue stress levels. This means that, in some cases, there is no advantage in using ECCs when the cross sectional area is scaled according to the static strength.

Figure 7 summarizes the evolution of midspan deflection at different fatigue stress levels, where one typical behavior is selected for each stress level. The

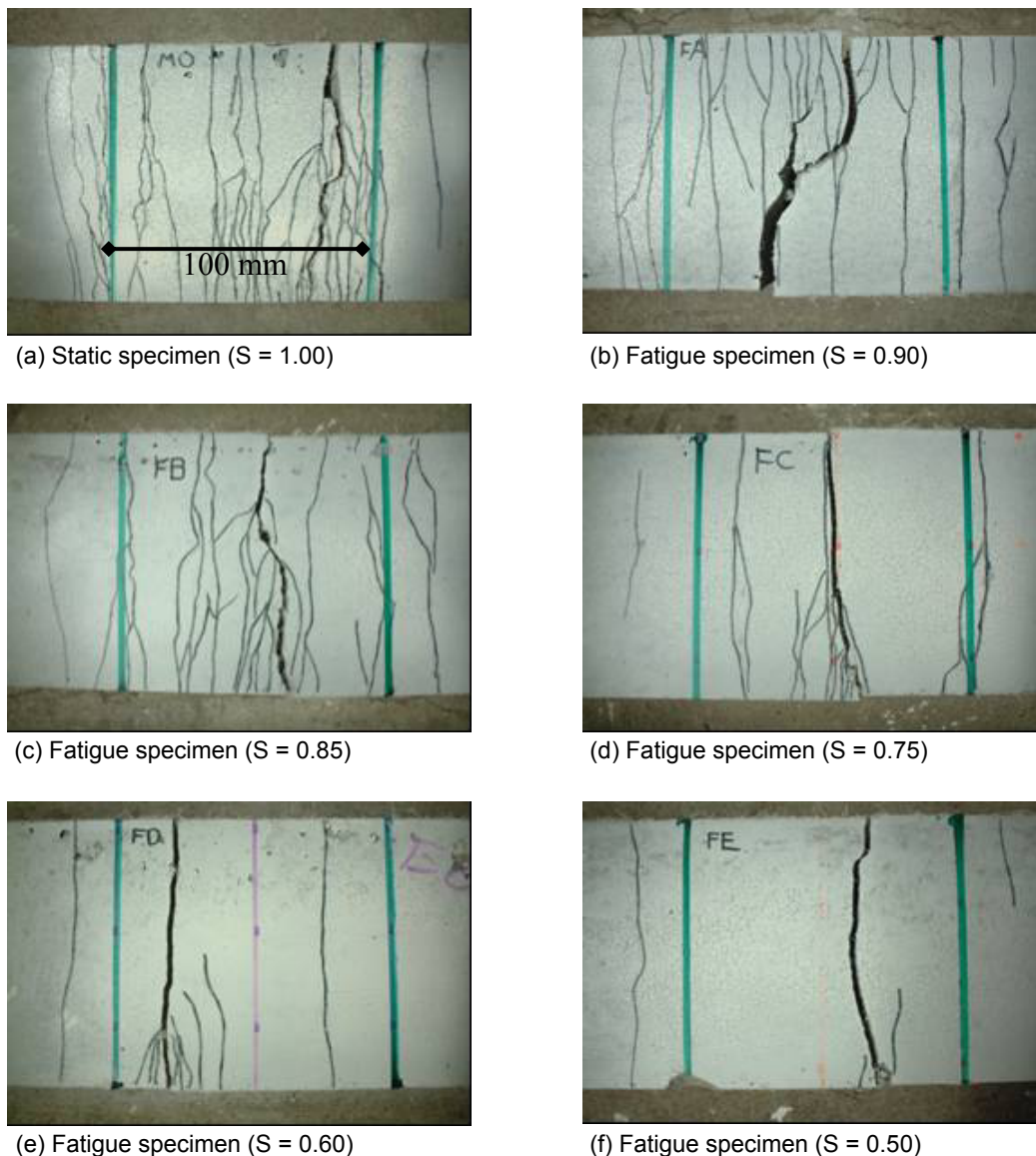


Fig. 3 Crack patterns on tension face of PVA-ECC beam specimens after failure.

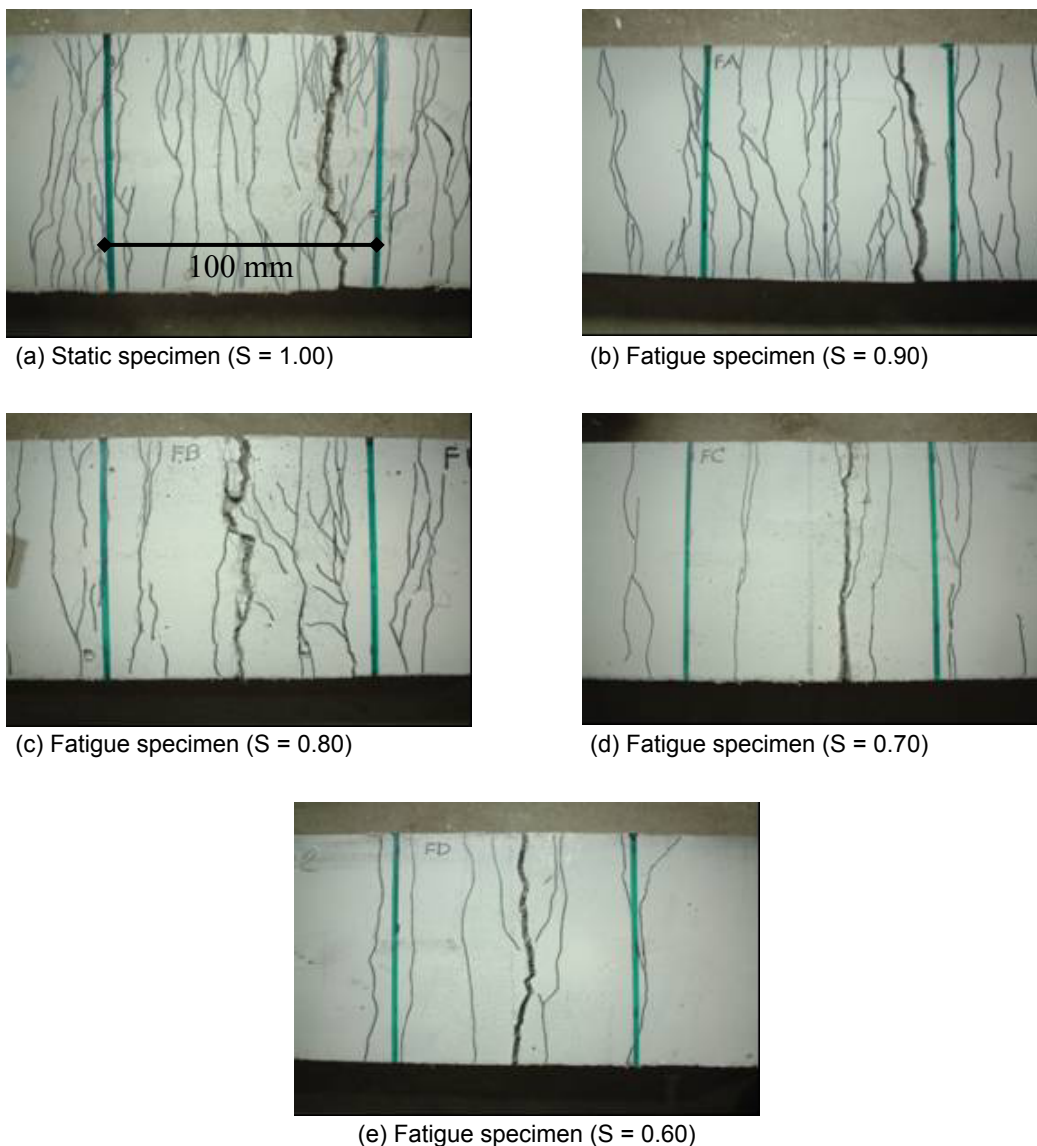


Fig. 4 Crack patterns on tension face of PE-ECC beam specimens after failure.

evolution can be divided into three phases: initial phase, steady state phase, and final phase. In the initial phase, multiple cracks that formed during the gradual load increase in the first cycle tended to grow. Some were visible from the beginning, and others became visible after their growth. Together with these preformed multiple cracks, new cracks were also created. All the cracks contributed to the initial rise of the midspan deflection. In the second phase, the formation of new cracks practically ceased, while the existing cracks gradually increased in length and width. This is presumably why the slope of deflection evolution became mild and steady. In the final phase, only one of the multiple cracks tended to open significantly, and it became the localized crack that caused specimen failure. The final rise of deflection could be attributed to the significant opening of the localized crack.

The evolution was dependent on the fatigue stress level. Namely, the midspan deflection increased more than twice under high fatigue stress levels ($S = 0.8$ to 0.9) compared to that under low stress levels ($S = 0.5$ to 0.6). It was also noticed that until the moment of final failure PVA-ECC generally deflected more than PE-ECC and that PVA-ECC had higher deformation capacity under fatigue loading. This is contrary to the fact that PE-ECC had higher deformation capacity under static loading. The mechanisms of the different behaviors will be discussed later.

Figure 3 shows the crack patterns on the tension face of PVA-ECC beam specimens after failure, and **Fig. 4** shows the same for PE-ECC beam specimens. One typical specimen is selected for each fatigue stress level. The middle third of the span is shown, and the line in (a) has a length of 100 mm. As can be seen in the photographs, these two ECCs exhibited multiple crack-

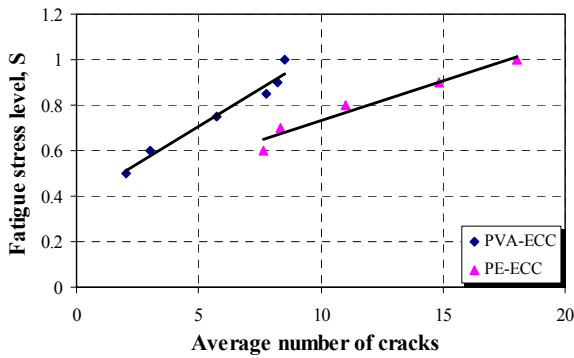


Fig. 5 Average number of cracks at different fatigue stress levels.

ing even under fatigue loading. Below, these crack patterns are evaluated from the viewpoint of fatigue stress levels and ECC types.

First, for both ECCs, cracking patterns and behaviors were dependent on fatigue stress levels. It was found that more cracks were formed at higher fatigue stress levels and unexpectedly that there were fewer cracks at lower fatigue stress levels. At $S = 0.8$ to 0.9 , a large number of cracks formed, and they contributed to larger deflection during fatigue loading, as shown in Fig. 7. By contrast, at $S = 0.5$ to 0.6 , only a small number of cracks were formed, meaning that ECCs tended to behave in a similar fashion to single cracking FRC. For example, the final deflection of both ECCs at $S = 0.5$ to 0.6 is within 0.5 mm and comparable to that of FRC.

Second, PE-ECC tended to crack more than PVA-ECC as in the case of static tests, and the crack widths of PE-ECC were smaller than PVA-ECC. This is clearly shown in Fig. 5, which plots the relationship between the average number of cracks and fatigue stress levels for two ECCs. However, it has to be mentioned again that a large number of cracks with small width did not increase deformation capacity in the case of fatigue.

In general, it was found that the final number of multiple cracks is different depending on the stress level and also that multiple cracking terminates earlier at

Table 5 Count of ruptured and pulled out fibers along arbitrary scan length of 10 mm on bottom and side edge of crack. A: B = ruptured fibers: pulled out fibers.

Material	Static	Fatigue
PVA-ECC	24 : 10	16 : 5
PE-ECC	17 : 31	13 : 22

lower stress levels.

4. Discussion

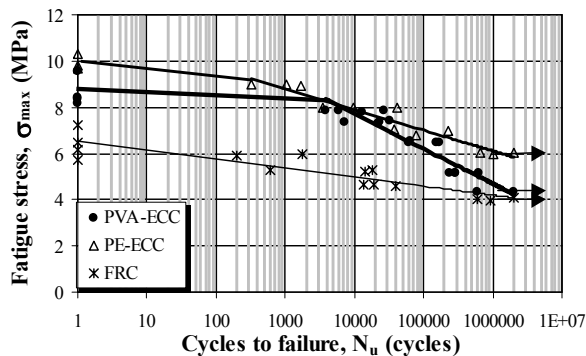
A discussion on multiple cracking and fracture of two ECCs follows based on the static and fatigue test results.

First, although ECCs showed multiple cracking under flexural fatigue loading as well as under static flexural loading, they did not exhibit extensive multiple cracking at lower fatigue stress levels. The number of cracks was significantly reduced at the lowest level in the tests, compared to the number of cracks at higher levels and under static loading. This is probably due to more severe multiple cracking condition under fatigue.

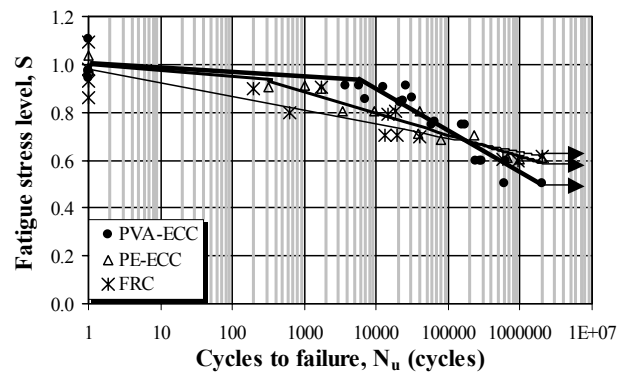
Under static loading, multiple cracks can be successively formed in such a way that the largest defect at the time starts to grow under increased external load. On the other hand, under fatigue loading, multiple cracks are formed at the first load application, and the number of cracks formed is dependent on the maximum fatigue stress level up to which the first load is increased. Therefore, the number of cracks is large at higher stress levels, and small at lower levels.

If the largest defect at the time starts to grow under an increased number of load repetitions, further multiple cracking can be expected even under fatigue loading. However, for this to take place under bridging stress degradation (Li et al. 1998), probably a more severe multiple cracking condition has to be met.

Second, PE-ECC showed a higher deformation capacity under static loading than PVA-ECC, but it showed a lower deformation capacity under fatigue

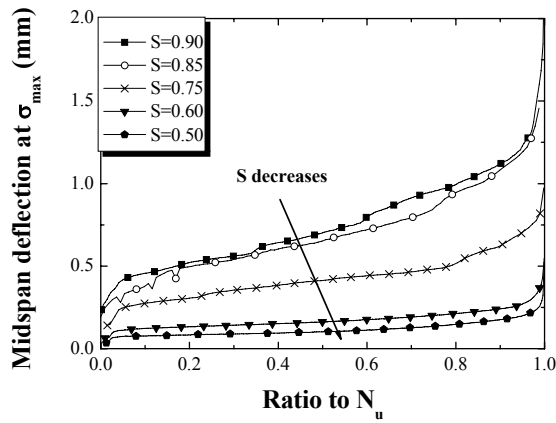


(a) Fatigue stress-life relationship

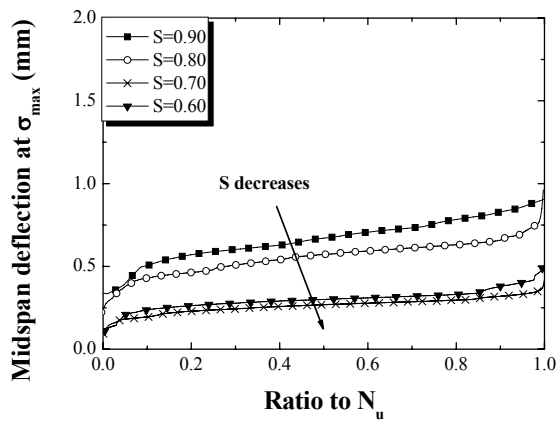


(b) Fatigue stress level-life relationship

Fig. 6 Stress-life (S-N) relationships of PVA-ECC, PE-ECC, and FRC.



(a) PVA-ECC



(b) PE-ECC

Fig.7 Evolution of midspan deflection at different fatigue stress levels.

loading. This can be explained by the opening behavior of cracks. **Figure 8** shows COD (Crack Opening Displacement) measurements at different fatigue stress levels. As the number of cycles increased, COD steadily increased, and it was found that PVA-ECC opened more than PE-ECC. This led to the deflection evolution of PVA-ECC under fatigue loading.

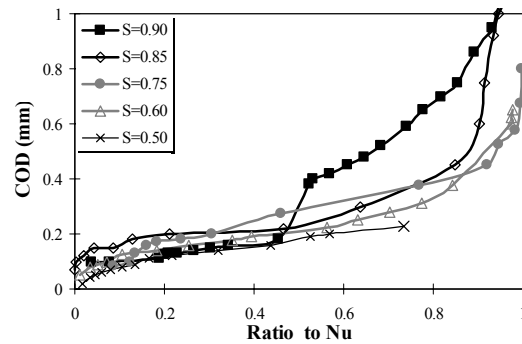
Finally, the difference in the fracture mechanism between PVA-ECC and PE-ECC is discussed based on microscopic observations. **Table 5** shows a brief summary of microscopic observations. Photographs of extruded fibers on the crack surfaces were taken, and the fiber tips were observed. Along an arbitrary scan length of 10 mm, the number of ruptured fibers and pulled-out fibers was counted on the bottom and side edges of static or fatigue specimens. The result shows that PVA fibers were severely ruptured under fatigue loading, while PE fibers suffered from rupture and pullout in similar proportions. Therefore, the aforementioned COD increase can be attributed to the decreasing number of fibers undergoing fatigue rupture.

5. Conclusions

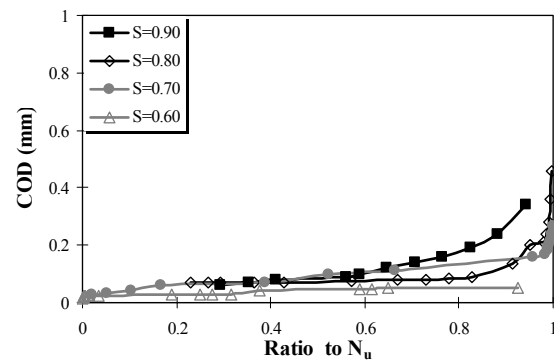
This paper showed fatigue test results of two types of ECCs: one reinforced with polyvinyl alcohol fibers (PVA-ECC) and the other with polyethylene fibers (PE-ECC). Eighteen specimens for PVA-ECC and 12 specimens for PE-ECC were tested under flexural fatigue. All the specimens were subjected to sinusoidal cyclic loading at the frequency of 8 Hz and with the ratio of the minimum stress level to the maximum stress level set to 0.2. Fatigue tests were conducted under five fatigue stress levels for PVA-ECC and four for PE-ECC, and the entire fatigue stress-life (S-N) relationships were constructed for the two ECCs.

The fatigue life of ECCs is superior to that of FRC. Their S-N relationship resembles that of metallic materials, and it can be characterized by a bi-linear relation on a semi-log plot. On the other hand, FRC exhibits a typical S-N relationship that is represented by a linear relation on the same plot. It was found that such a unique S-N relation is due to the fact that ECCs recorded relatively longer fatigue life at higher fatigue stress levels. However, it was also found that the fatigue life of ECCs tended to be equivalent or shorter than that of FRC at lower fatigue stress levels.

The midspan deflection evolution can be divided into three phases: initial phase, steady state phase, and final



(a) PVA-ECC



(b) PE-ECC

Fig. 8 COD measurement during fatigue loading.

phase. These phases are closely related to multiple crack occurrences and growth. Multiple cracks were found to take place under fatigue loading, however their development was significantly dependent on fatigue stress levels. At high stress levels, a large number of cracks were formed, and they contributed to larger deflection during fatigue loading. By contrast, at low stress levels, only a small number of cracks were formed, meaning that ECCs tended to behave in a similar fashion to single cracking FRC.

PVA-ECC showed higher deformation capacity under fatigue loading than PE-ECC, although PE-ECC tended to crack more than PVA-ECC as in the case of static tests, and the crack widths of PE-ECC were smaller than PVA-ECC. This is because of the higher opening tendency for each of the cracks, and, in this case, the tendency is attributed to the fatigue rupture of bridging fibers.

Acknowledgments

Helpful discussions with Dr. H. Horii and Dr. V. C. Li are gratefully acknowledged. Matsumoto and Suthiwarapirak are indebted to Kajima Technical Research Institute for providing them experimental specimens.

References

- JCI-SF4 (1984). "JCI Standards for Test Methods of Fiber Reinforced Concrete." Japan Concrete Institute, Tokyo, Japan, 45-48.
- Kanda, T. and Li, V. C. (1999). "New micromechanics design theory for pseudo strain hardening cementitious composite." *ASCE J. of Engineering Mechanics*, 125 (4), 373-381.
- Kanda, T. and Li, V. C. (2001a). "Practical design guidelines for pseudo strain hardening cementitious composites reinforced with short random fibers -Part I Micromechanics theory for predicting first cracking strength-." *J. Struct. Constr. Eng., AIJ* (539), 13-21 (in Japanese).
- Kanda, T., Saito, T., Sakata, N. and Hiraishi, M. (2001b). "Fundamental properties of directed sprayed retrofit material utilizing fiber reinforced pseudo strain hardening cementitious composites." *Proceedings of the Japan Concrete Institute*, 23 (1), 475-480 (in Japanese).
- Li, V. C. and Wu, H. C. (1992). "Conditions for pseudo strain-hardening in fiber reinforced brittle matrix composites." *ASCE J. of Applied Mechanics Review*, 45 (8), 390-398.
- Li, V. C. and Matsumoto, T. (1998). "Fatigue crack growth analysis of fiber reinforced concrete with effect of interfacial bond degradation." *Journal of Cement and Concrete Composites*, 20 (5), 339-351.
- Maalej, M. and Li, V. C. (1994). "Flexural/tensile strength ratio in engineered cementitious composites." *ASCE J. of Materials in Civil Engineering*, 6 (4), 513-528.
- Rokugo, K. and Fukuyama, H. (2002). "Preface." *Proceedings of the JCI International Workshop on Ductile Fiber Reinforced Cementitious Composites - Application and Evaluation-*, i-ii.
- Suthiwarapirak, P. and Matsumoto, T. (2002). "Flexural fatigue failure characteristics of engineered cementitious composites." *JSCE J. of Materials, Conc. Struc. Pavement*, 718 (57), 121-134.